ACADEMIA ROMÂNĂ
Revue Roumaine de Chimie
https://www.icf.ro/rrch/

Rev. Roum. Chim.,
2024, *69*(7–8), 423–432
DOI: 10.33224/rrch.2024.69.7-8.10

MAGNETIC MICRO SOLID-PHASE EXTRACTION FOR A NOVEL UHPLC-DAD METHOD FOR THE DETERMINATION OF ATOMOXETINE (ATX) IN BREAST MILK AND HUMAN PLASMA

Burhan CEYLAN,[a,*] Nurdan KURNAZ YETİM,[b] Cemile ÖZCAN,[b]
Mümin Mehmet KOÇ[c,d] and Cem ÖNAL[e]

[a]Department of Pharmacognosy, Faculty of Pharmacy, Harran University, Sanlıurfa, Turkiye
[b]Department of Chemistry, Faculty of Arts and Sciences, Kırklareli University, Kırklareli, Turkiye
[c]Department of Health Service and Techniques, School of Medical Service, Kırklareli University, Kırklareli, Turkiye
[d]Department of Physics, Faculty of Arts and Sciences, Kırklareli University, Kırklareli, Turkiye
[e]Department of Analytical Chemistry, Faculty of Pharmacy, Istanbul Health and Technology University, Istanbul, Turkiye

Received March 13, 2024

Atomoxetine is a special pharmaceutics used for attention deficit hyperactivity disorder. It finds application in various age groups, including children, adolescents, and adults. Ultra high-performance liquid chromatographic technique (UHPLC) is an exceptional technique and provides swift, uncomplicated, and highly sensitive results. Such a technique has been formulated to analyse atomoxetine levels in both breast milk and human plasma. Magnetic micro solid phase extraction is simple, rapid, efficient, and precise method which was applied prior to chromatographic separation. In this method, magnetic adsorbents in the form of Fe_3O_4 magnetic nanoparticles were employed, and the adsorption process underwent optimization. Chromatographic separation was carried out using a reversed-phase C18 analytical column (5 µm × 4.6 mm × 150 mm) with a mobile phase composed of monobasic potassium dihydrogen orthophosphate (pH=6.8) and acetonitrile (50:50 v/v). The flow rate was set at 0.8 mL/min, and investigation was performed using DAD at 215±2 nm. The method's linearity was evaluated within the range of 0.5–20 µg/mL, achieving a correlation coefficient (*r*) of 0.999. Validation of the method encompassed accuracy, reproducibility, precision, robustness, specificity, quantification limits, and detection limits, adhering to EMA guidelines. The limit of detection (LOD) was found to be 0.03, while the limit of quantification (LOQ) was 0.11 µg/mL for both matrices. Interday and intraday relative standard deviation (RSD) values were determined to be below 2.5% for both assays. The suggested method is deemed to be a useful candidate for the conventional quantification of atomoxetine in human spiked breast milk and plasma.

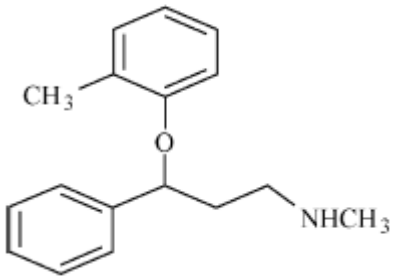

INTRODUCTION

Attention deficit hyperactivity disorder (ADHD) is a neurodevelopmental condition diagnosed by executive dysfunction, resulting in symptoms of inattention, hyperactivity, impulsivity, and emotional dysregulation. These symptoms are excessive and pervasive, impairing individuals in various contexts. The disorder affects quite large number of children of children and adolescents worldwide (approx. 5–12%). It is linked to significant morbidity and predicts poorer outcomes later in life, making it the most commonly diagnosed and treated mental disorder in children.[1,2] Atomoxetine hydrochloride

* Corresponding author: b.ceylan022@gmail.com.

(ATX) is the first non-stimulant, orally administered, selective norepinephrine reuptake inhibitor (see Fig. 1 for the chemical structure). ATX is approved by the United States Food and Drug Administration (FDA) in 2002 for treating ADHD in individuals aged 6 years or older.[3,4]

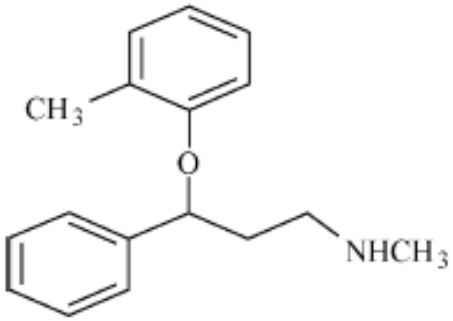

Fig. 1 – Chemical structure of ATX.

The specific mechanism through which ATX exerts its therapeutic effects in patients with ADHD remains undiscovered. ATX boosts norepinephrine function by specifically inhibiting the presynaptic norepinephrine transporter, demonstrating minimal affinity for other neuronal transporters and/or neurotransmitter receptors. This process leads to an increased norepinephrine concentration. Enhanced norepinephrine functions at the inter-neuron connections in the brain.[5–7] Studies conducted with ATX in healthy volunteers displayed a bimodal distribution in ATX clearance, hinting at the participation of an enzyme with a genetic polymorphism in ATX metabolism.[8]

Blood, plasma, serum, and breast milk are common matrix is used for therapeutic drug monitoring. Humans breast milk is a superior source of nutrition for the babies. It was strongly advised by clinicians for the first six months of newborns. It is not only a food source for babies but also a special ritual with several health and social benefits. While breast milk is the best nutritional choice for infants, those who are breastfed may encounter medications from their mothers' treatment. Hence, it is essential to evaluate the quantity of medication transferred to the milk and comprehend the potential impact of this exposure on the infant's development.[9,10] There is a noticeable lack of research in existing literature regarding the analysis pertaining the determination of ATX in breast milk. Previously, some studies pertaining the determination of ATX in human plasma were reported.[11-23] Current methods are not preferred because they are expensive, require long method preparation, and are not sensitive enough. However, investigated reports do not illustrate UHPLC-DAD and magnetic micro-solid phase extraction (M-μ-SPE) methods.

In this work, an UHPLC technique was demonstrated to analyse ATX in μg/mL level in breast milk and human plasma with diode array detector (DAD) detection. Human plasma and breast milk are complex matrix. Thus, magnetic micro-solid phase extraction is applied as pretreatment. Compared to liquid-liquid extraction (LLE), M-μ-SPE is found to be a simpler method. Moreover, M-μ-SPE is cost effective due to reduced solvent consumption, rapid and facile processing. In the presented work, a facile analytical method, M-μ-SPE combined with UHPLC, has studied for determination of ATX in breast milk and human plasma.

EXPERIMENTAL

Apparatus

Different methods were utilized for the structural and morphological assessment of the extraction sorbents. These are energy dispersive X-ray spectroscopy (EDS), X-ray diffractometry (XRD), Fourier transform infrared spectroscopy (FTIR), high resolution transmission electron microscopy (HR-TEM), and scanning electron microscopy (SEM). A Rigaku X-ray diffractometer was utilized (with Cu-Kα radiation) to obtain XRD patterns, which were then employed to assess the crystalline size and crystal structure. A Bruker ATR- FTIR spectrometer were used to obtain the FTIR spectra of MNPs in the range of 400-4000 cm^{-1}. A LDJ Electronics Inc., Model 9600 vibrating sample magnetometer were used to investigate the magnetic characteristics of MNPs. Magnetic characterization was conducted at room temperature. FEI Tecnai G2 Sphera microscope was utilized for the transmission electron microscopy (TEM) investigations. For the TEM analysis, MNPs are diluted in ethyl alcohol and a drop of diluted sample drop cast on a TEM grid. FEI quanta FEG 250 was used for the scanning macroscopy investigations; EDX apparatus of the SEM was used for the elemental analysis. WTW pH 526 digital pH Meter was used for the pH analysis. Agilent 1260

Infinity HPLC-DAD was used for assessment and detection of ATX in human plasma and breast milk. Phenomenex-C18 (5 μm × 4.6 mm × 150 mm) column was used for the chromatography. Millipore Direct-Q water purification tool was used to obtain pure water.

Chemicals and Solution

All substances utilized in this study are of analytical grade and were obtained from Merck (Germany) which are ammonia solution 28% (NH_3), iron(II) chloride tetrahydrate ($FeCl_2.4H_2O$), tetraethyl orthosilicate (TEOS), iron(III) chloride hexahydrate ($FeCl_3.6H_2O$). Chemicals were used as purchased, without any additional purification or refining processes.

Shanghai Yingxuan Pharmaceutical Science & Technology (China) provided the ATX used in our assessments. 100 mg ATX containing Strattera® capsules were bought from local drug store. Phosphate buffer, acetonitrile, and NaOH were HPLC grade. Free base calculated ATX containing 200 μg/mL stock solution was prepared in water.

The initial solution was diluted to create a standard solution: Such a dilution yielded solutions in the range of 0.5 to 20 μg/mL.

Synthesis of Fe_3O_4@SiO_2 Nanoparticles

Prior to production of silica coated magnetic nanoparticles, Fe_3O_4 nanoparticles were produced using coprecipitation method. For this purpose, 1 g $FeCl_2.4H_2O$ and 2.6 g $FeCl_3.6H_2O$ and 25 mL of pure water were added in a flat bottom bubble. The mixture was stirred until $FeCl_2.4H_2O$ and $FeCl_3.6H_2O$ were totally dissolved. Then, 28% NH_3 solution was dropwisely added to the mixture. Result product was magnetically stirred at 60 ºC for 2 h. A neodymium magnet was used for the collection of magnetic nanoparticles. Powder like magnetic nanoparticles were washed twice with pure water. Then washed nanoparticles were ethanol washed and placed in a vacuum oven for 24h. The inner temperature of the vacuum oven was 40 ºC.[24–26] For the TEOS coating process, 0.1 mg magnetic nanoparticle powder was mixed with 20mL ethyl alcohol. Suspension was sonicated for 25 min; 1mL TEOS and 1mL 28% NH_3 solution was dropwisely added to the suspension. The mixture was transferred to the magnetically stirrer and stirred there for 12 h. Preparation process was conducted at room temperature. MNPs were retrieved using a neodymium magnet and underwent two rounds of washing with water and ethanol. The resulting powder-like nanoparticles were kept at vacuum oven 24 h.[27]

Sample Preparation

To take the blood samples ethical committee approval was obtained. Investigated blood samples were obtained from a volunteer's peripheral veins. Consent of the donors were obtained. The samples were stored in disodium EDTA containing falcons. To obtain human plasma, blood samples were centrifuged at 4500 x g for 10 minutes. The resulting plasma samples were kept in deep freezer. Plasma samples stored at –22 ºC. Similarly, samples of breast milk were obtained from a volunteer mother aged 25, with her informed consent obtained after ethical committee approval. These milk samples were collected into polyethylene storage packs. The resulting plasma samples were also transferred to the deep freezer, and they stored at –22 ºC. The M-μ-SPE technique was applied to extract the ATX from both the milk and plasma. In this process, 75 milligrams of Fe_3O_4 MNPs were introduced to 1 mL of both milk samples and plasma samples. The mixture was stirred using a vortex mixer for 15 minutes. Using a magnet, the magnetic nanoparticles were collected, allowing for easy removal of the supernatant. Subsequently, Fe_3O_4 nanoparticles were washed with 1 mL acetonitrile to clean nanoparticles where drug was eluted with the solvent. Since iron oxide nanoparticles are highly magnetic, they have tendency to agglomerate. Therefore, filtration process was applied to the suspension. In this process, 0.45 mm filter was used get rid of a potential agglomeration. The filtered result product in acetonitrile (20 μL) was transferred to the HPLC system. To obtain the higher recovery rate, optimum conditions for desorption solvent type, pH, volume of extracted human plasma, amount of desorption solvent, volume of extracted milk, magnetite amount, mixing time were determined.

RESULTS AND DISCUSSION

Structural and morphological investigation of Fe_3O_4@SiO_2 nanoparticles

X-ray diffraction patterns of Fe_3O_4 magnetic nanoparticles and Fe_3O_4@SiO_2 magnetic composites were presented in Fig. 1 where samples were scanned between 0˚ and 80˚ for 2θ. Diffraction pattern belonging to Fe_3O_4 exhibits peaks at 78.94˚, 74.98˚, 74.12˚, 70.98˚, 62.8˚, 57.3˚, 53.36˚, 43.3˚, 37.08˚, 35.6˚, 30.4˚ and 18.3˚. Mentioned peaks illustrate that iron oxide nanoparticles exhibit face centred cubic (fcc) formation characteristics in (4 4 4), (6 2 2), (5 3 3), (6 2 0), (4 4 0), (5 1 1), (4 2 2), (4 0 0), (2 2 2), (3 1 1), (2 2 0) and (1 1 1) direction, respectively.[27] Sharp peaks in the diffraction pattern illustrate that nanoparticles produced using coprecipitation method are pure and well crystallized. Silica coated magnetic nanoparticles exhibit broad peaks which are similar to iron oxide nanoparticles in fcc structure in (2 2 0), (3 1 1), (4 0 0), (4 2 2), (5 1 1), (4 4 0), (6 2 0), (5 3 3), (6 2 2) and (4 4 4) directions. It was concluded that silica coat over the iron oxide nanoparticles shadows the collected date where broadened peaks were observed. No apparent silica crystal related peak observed such a case illustrates that silicon atoms in TEOS coat are not crystallized and possible stayed in amorphous form. It was also concluded that silicon atoms in TEOS do not forma crystal structure with iron oxide nanoparticles were nanoparticles where no additional Si-Fe related peak was observed.[26]

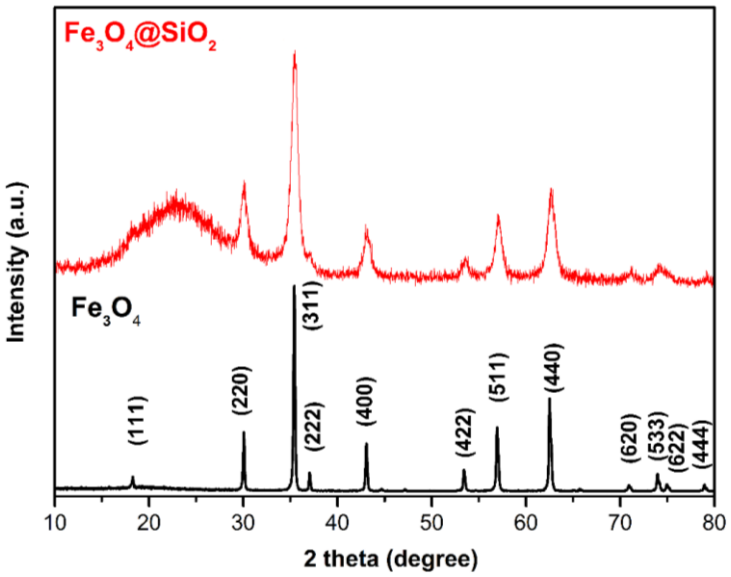

Fig. 2 – XRD pattern of Fe_3O_4 and $Fe_3O_4@SiO_2$ magnetic nanoparticles.

To investigate the chemical composition of iron oxide nanoparticles and magnetic nanocomposites FTIR spectra of the samples were investigated. FTIR spectra of samples were presented in Fig. 3. FTR spectrum of Fe_30_4magnetic nanoparticles exhibit a band at 583cm^{-1} and 456 cm^{-1} that were attributed to Fetetra↔O and Feocta↔O stretching vibrations occur in tetrahedral and octahedral zones, respectively.[24-26]

The band seen at 562 cm^{-1} for $Fe_3O_4@SiO_2$ magnetic nanocomposites was attributed to Fe-O tension vibration. The mentioned band is a characteristics band illustrating the Fe-O tension which was also seen at 558 cm^{-1} for pure Fe_3O_4 nanoparticles. A slight shift was associated with silica based TEOS cover. Bands seen at 1053 cm^{-1}, 948 cm^{-1}, and 795 cm^{-1}are corresponding the Si-O-Si asymmetrical vibrations. Such bands confirms that Fe_3O_4 nanoparticles are successfully covered with TEOS where SiO_2 based cover was obtained.[28]

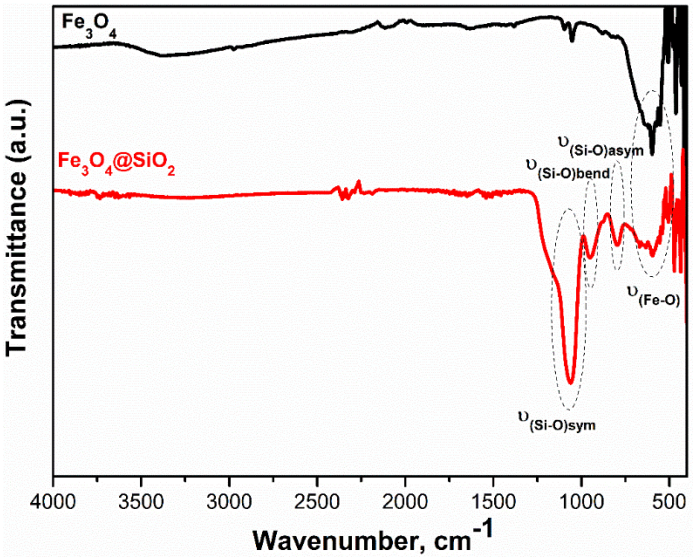

Fig. 3 – FTIR spectra of Fe_3O_4 magnetic nanoparticles and $Fe_3O_4@SiO_2$ magnetic nanocomposites.

SEM images and EDX spectra of Fe_3O_4 magnetic nanoparticles and $Fe_3O_4@SiO_2$ magnetic nanocomposites were illustrated in Fig. 4 and Fig. 5, respectively. SEM images of Fe_3O_4 magnetic nanoparticles illustrate that nanoparticles are quite small and agglomerated and form a big lumpy structure. It was concluded that such an agglomeration was occurred due to the magnetic

characteristics of the nanoparticles. EDX spectrum of the Fe_3O_4 magnetic nanoparticles were presented below the SEM image where peaks belonging Fe and O atoms could be identified. No contamination related peaks were observed in the EDX spectrum which illustrate that nanoparticles are highly pure.

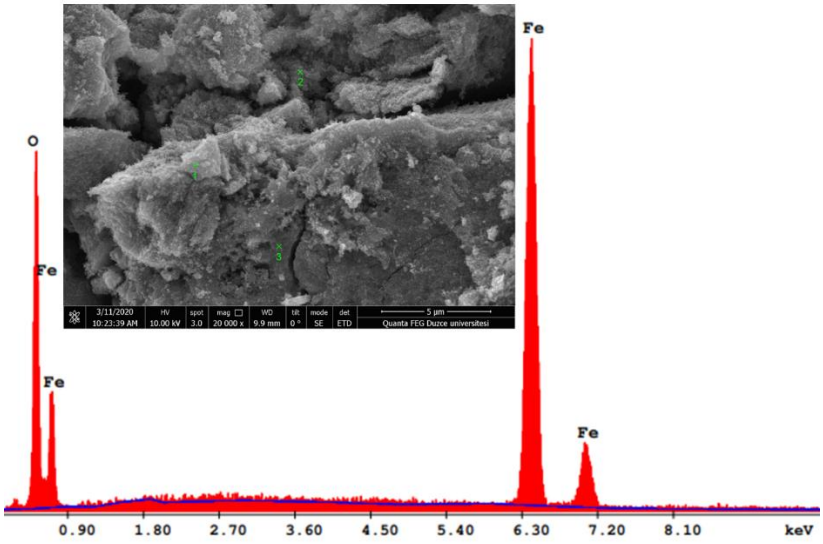

Fig. 4 – SEM image and EDX spectrum Fe_3O_4.

SEM image of $Fe_3O_4@SiO_2$ magnetic nanocomposites exhibit slightly different characteristics compared to the pure iron oxide nanoparticles. Spherical lumps could be identified but lumpy structures were found to be in granulated forms. Small granules could be identified. EDX spectrums obtained from the region where is marked as 2. EDX spectrum exhibit Si, O and FE atom related peaks. The peaks were found to be quite sharp, and no contamination related peaks were observed. It was concluded that $Fe_3O_4@SiO_2$ nanocomposites are quite pure are not contaminated.

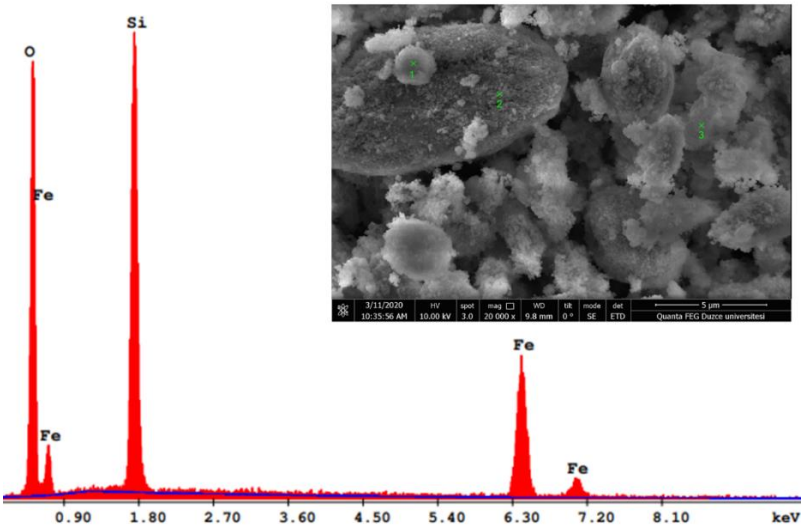

Fig. 5 – SEM image and EDX spectrum of $Fe_3O_4@SiO_2$ magnetic nanocomposites.

Figure 6 illustrates TEM images of Fe_3O_4 magnetic nanoparticles (a) and $Fe_3O_4@SiO_2$ magnetic nanocomposites (b). Size of Fe_3O_4 magnetic nanoparticles were found to be around 10–15 nm. TEM images also confirms that Fe_3O_4 magnetic nanoparticles has agglomeration tendencies. Size of $Fe_3O_4@SiO_2$ magnetic nanocomposites were found to be slightly bigger around 30–40 nm. It was seen that nanoparticles were coated with a coat. Since atomic weight of iron is higher than Si, Fe_3O_4 nanoparticles could be identified inside the Si based shell. Si shell could

successfully cover the surface of the Fe_3O_4 nanoparticles. TEM images confirms that nanocomposites are in core@shell structure which supports our claims.

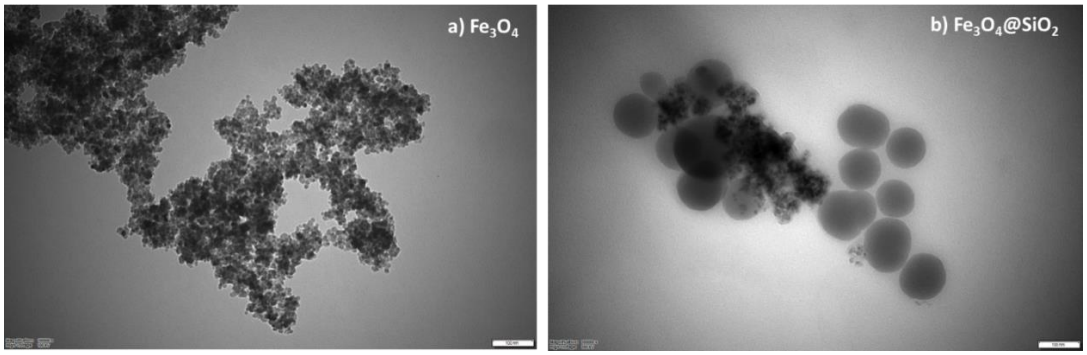

Fig. 6 – TEM images of pure Fe_3O_4 magnetic nanoparticles (a) and Fe_3O_4@SiO_2 (b) magnetic nanocomposites.

Magnetic characteristics of the magnetic nanoparticles and magnetic nanocomposites were investigated. Vibrating sample magnetometry (VSM) was used in the magnetic characterization; the characterization process was conducted between –1.5T and +1.5T. Magnetic hysteresis plots of Fe_3O_4andFe_3O_4@SiO_2magnetic nanoparticles were presented in Fig. 7. Magnetic hysteresis characteristics of the Fe_3O_4@SiO_2nanocomposites and Fe_3O_4 magnetic nanoparticles illustrate that both Fe_3O_4 magnetic nanoparticles and Fe_3O_4@SiO_2magnetic nanocomposites exhibit superparamagnetic characteristics. They have quite small magnetic coercivity which could not be identified in the plots. Magnetic saturation value of Fe_3O_4 magnetic nanoparticles were determined to be 63.7 emu/g. The result was found to be aligning with findings reported in existing literature. The magnetic saturation of the Fe_3O_4@SiO_2 magnetic nanocomposites were found as 23.9 emu/gr. It was seen that covering Fe_3O_4 nanoparticles with TEOS cover slightly decrease the magnetic saturation value. The case is quite common in the literature where most of reports support similar case. Surprisingly magnetic characteristics of the nanoparticles were not altered after TEOS coat where both Fe_3O_4 magnetic nanoparticles and Fe_3O_4@SiO_2 magnetic nanocomposites exhibit superparamagnetic characteristics.[27]

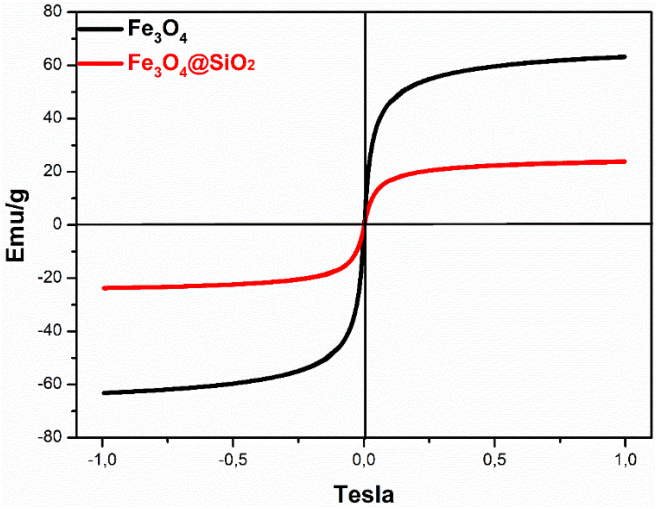

Fig. 7 – Magnetic hysteresis plots of pure Fe_3O_4 nanoparticles and Fe_3O_4@SiO_2 magnetic nanocomposites.

Optimization of (M-μ-SPE) parameters

Different parameters such as volume of extracted human plasma, volume of extracted breast milk, pH, stirring time, the type of desorption solvent and amount of desorption solvent were investigated. 0.1 M of NaOH solution (pH = 6.8) and 20 mM of phosphate buffer stock (pH = 3.3) were used for the adjustment of the acidic and alkaline media. It was seen that the adsorption efficiency in the acidic and alkaline media

was lower than that the adsorption efficiency in the plasma (pH = 7.4). Thus, it is slightly easier to work in the plasma without altering the pH. Our assessments about nanoparticle amount was conducted between 5mg and 150mg; it was revealed that optimum amount of MNP is 75 mg. The optimum extraction volume was found to be 5 mL, and the optimum mixing time was found to be 1 minute. These values were determined after checking the experimental ranges of 0.1 to 5.0 mL for volume and 1 to 5 minutes for mixing time. This optimization ensures minimal solvent consumption and facilitates a swift extraction process. Various solvents were tested in the study such as including ethanol, ethyl acetate, methanol, acetone, and acetonitrile; it is concluded that acetonitrile was the most prominent solvent. It provides the highest recovery for the desorption. Acetonitrile served as the mobile phase in the chromatographic analyses, and a sufficient recovery was achieved using just 1 mL of the solvent.

Chromatographic investigations

To achieve optimum conditions, different mobile phase, column size and column types were assessed. Tests were conducted for various column temperatures and flow rates. Reversed phase (RP) HPLC was chosen in our investigations where column (Phenomenex-C18, 5 μm × 4.6 mm × 150 mm) was used. The mobile phase was acetonitrile-monobasic potassium dihydrogen orthophosphate (pH = 6.8) (50:50 v/v) with a flow rate of 0.8 mL/min were used with isocratic elution characteristics. For optimum chromatogram resolution, investigations were performed at 30ºC column temperature. The retention time is about 1.346 ± 0.004 min. The chromatograms for 10 μg/mL ATX in breast milk samples, human plasma samples, blank breast milk samples and blank human plasma samples are shown in Fig. 8.

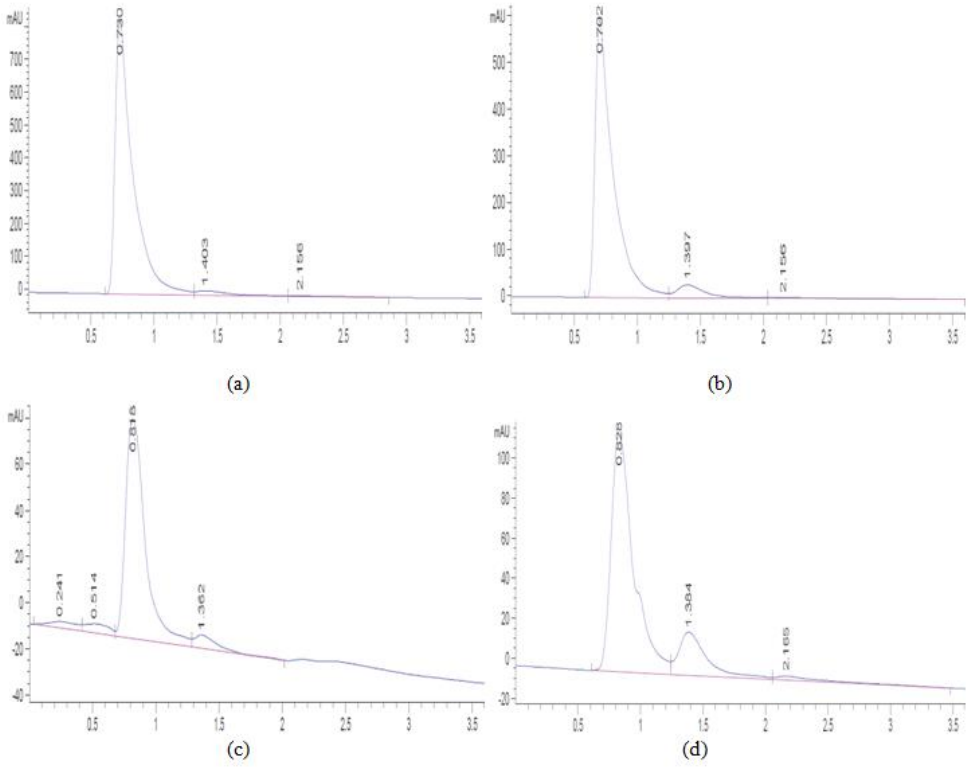

Fig. 8 – a) Blank breast milk (placebo breast milk); b) 10 μg/mL ATX spiked to breast milk; c) blank plasma (placebo plasma); d) 10 μg/mL ATX spiked to plasma.

Method validation

To verify the new method, different guidelines which obey the European Medical Agency (EMA) were used.[29] In this regard, parameters such as; sensitivity, stability, linearity, precision and accuracy, and robustness were tested.

Precission and accuracy

Accuracy and precission and were assessed by analysing quality control (QC) samples for different concentrations (2.5, 5.0, and 10 μg/mL) which represent low, moderate, and high concentrations for each matrix.

The accuracy evaluation was employed to the recovery method, and precision was gauged based on intraday and interday relative standard deviation (RSD) values. The accuracy of the method was assessed through the standard addition approach. In the standard addition approach, QC samples of standard drug solutions were added to milk and plasma at a concentration of 10 μg/mL of ATX. Recovery rates were determined using the formula: Recovery % = $[(Con_t–Con_u)/Con_a]\times100$, where Con_a is the concentration of the added standard drug, Con_u is the analyte concentration in the formulation, and Con_t is the total analyte concentration. The calculated recovery values were %105.22 and %100.35, with corresponding RSDs of 0.67 and 0.35 for milk and plasma.

To assess precision, interday and intraday repeatability were scrutinized by determining RSD. Five samples replicates at each concentration were analysed on the same day for intraday precision and on three separate days for interday precision. The RSD values for both intraday and interday analyses consistently remained below 1.27%. These results signify that the proposed method exhibits exceptional precision and accuracy. A detailed results pertaining experimental findings is presented in Table 1.

Table 1

The results pertaining to precision and accuracy studies

	Existent concentration (μg mL^{-1})	Added concentration (μg mL^{-1})	Found concentration (μg mL^{-1}) (Mean±SD[1])	Recovery (%)	RSD of recovery	RSD of intraday variation	RSD of interday variation
Plasma	10	2.5	12.48	99.86	0.35	0.35	0.39
		5.0	15.01	100.08	0.32	0.32	0.36
		10.0	20.07	100.35	0.27	0.27	0.33
Breast milk	1	2.5	3.52	100.51	0.67	0.67	1.27
		5.0	6.31	105.22	0.18	0.18	0.38
		10.0	11.24	102.21	0.36	0.36	0.78
Mean relative recovery = 102.38							

$n = 5$

Sensitivity and linearity

Linear least-squares regression analysis was used to generate calibration curves. In this regard, graphs were generated by plotting the peak areas of the derivatives against the respective concentrations of ATX. The calibration curve, derived from five points, is expressed as $y = 102.8x – 5.101$, with a correlation coefficient of 0.9990 (where $n = 5$). Here, x denotes the concentration of ATX, and y denotes the peak area of ATX. The technique demonstrates a linear relationship within the 0.5-20 μg/mL range. Table 2 summarizes the parameters about the results. The limits of quantitation (LOQ) and the limit of detection (LOD) values were calculated using the formula: LOQ or LOD = kSDa/b, where k =10 for LOQ and k =3 for LOD. SDa denotes the standard deviation of the intercept, while b denotes the slope. LOQ and LOD are presented in Table 2 as 0.11 μg/mL and 0.03 μg/mL, respectively.

Table 2

Analytical parameters obtained using proposed method

Parameters	**Method**
Regression equation[b]	$y = 102.8x – 5.101$
Concentration range [a] (μg mL^{-1})	0.5–20.0
Correlation coefficient (r^2)	0.9990
Slope± SD	102.8 ± 9.22
Intercept± SD	5.101 ± 0.457
LOD (μg mL^{-1})	0.03
LOQ (μg mL^{-1})	0.11

[a] Average of three analysis.
[b] $y = xC + b$ where C is the concentration in μg/mL and y is the peak area.

Robustness

Robustness was assessed by introducing slight modifications to column oven temperature, the flow rate, and the composition of water and acetonitrile in the mobile phase. The original mobile phase composition of (50:50 v/v) acetonitrile-phosphate buffer was adjusted to 45:55 and 55:45. Furthermore, variations were made to the column temperature, ranging from 30ºC to 25ºC and at 35ºC. The flow rate was modified from 0.7 to 0.9 mL/min. Importantly, such adjustments did not have a significant impact on the peak areas. Detailed results of the robustness tests can be found in Table 3. The recovery% values are better than the values in our previous study.[30]

Stability

The influence of deep freezing and the effect of thawing on ATX were examined by incorporating spiked QC samples of ATX in breast milk and plasma. ATX stability was tested at room temperature for 6 hours in breast milk and 24 h in plasma at –22ºC for a period of 4 weeks.

Table 3

Results from robustness experiments.

Condition	Value	Recovery (%)		RSD (%)	
		Plasma	Breast milk	Plasma	Breast milk
Flow rate mL/min	0.7	103.73	102.38	1.54	1.65
	0.9	98.32	99.49	1.35	1.45
Mobile phase composition (ACN: Phosphate buffer)	45:55	101.06	100.89	1.25	1.18
	55:45	99.75	100.08	0.88	1.41
Column temperature	25	100.56	99.66	0.94	1.35
	35	100.34	100.05	1.21	1.42

n =5

CONCLUSIONS

In this work, a novel approach for preparing and quantifying samples was studied to detect ATX in human breast milk and plasma. Both breast milk and plasma are sophisticated biological substances, with the latter containing diverse components such as considerable amount of water proteins, prebiotics, vitamins, and fats. The extraction of analytes from these matrices from breast milk and plasma, poses a significant challenge. The research focus on the M-µ-SPE technique with Fe_3O_4 as an adsorbent, achieving notable recoveries quickly and with a straightforward procedure. Especially in drug analysis, this technique emerges as a straightforward and effective alternative to traditional Liquid-Liquid Extraction and Solid-Phase Extraction. The adoption of M-µ-SPE stands out as a key advantage of the proposed method.

Moreover, the Reverse Phase High-Performance Liquid Chromatography part of the method is facile and does not demand advanced equipment or skilled operators, in contrast to tandem MS. Laboratories lacking access to such advanced tools can still apply this method. The mobile phase is not found to be complex, and there is no need for gradient elution; isocratic elution suffices, with a remarkably short retention time of approximately 1.34 min. The method demonstrates notable repeatability and accuracy.

REFERENCES

1. M. Dulcan, *J. Am. Acad. Child Adolesc. Psychiatr.*, **1997,** *36*, 85–121.
2. G. Polanczyk, M. S. Lima, B. L. Horta, J. Biederman and L. A. Rohde, *Am. J. Psychiatr.*, **2007,** *164*, 942–948.
3. F. A. Baughman, *JAMA*, **1999,** *281*, 780–788.
4. D. Michelson, D. Faries, J. Wernicke, D. Kelsey, K. Kendrick, F. R. Salle and T. Spencer, *Pediatrics*, **2001,** *108*, E83.
5. D. Michelson, L. Adler, T. Spencer, F. W. Reimherr, S. A. West, A. J. Allen, D. Kelsey, J. Wernicke, A. Dietrich and D. Milton, *Biol. Psychiatr.*, **2003,** *53*, 112–120.
6. E. Davids and M. Gastpar, *Fortschr Neurol Psychiatr.*, **2004,** *72*, 586–891.
7. A. K. Christman, J. D. Fermo and J. S. Markowitz, *Pharmacotherap.*, **2004,** *24*, 1020–1036.
8. J.-M. Sauer, G. D. Ponsler, E. L. Mattiuz, A. J. Long, J. W. Witcher, H. R. Thomasson, K. A. Desante, *Drug Metab. Dispos.*, **2003,** *31*, 98–107.
9. J. Raisler, C. Alexander and P. O'Campo, *Am. J. Public. Health.*, **1999,** *89*, 25–30.
10. B. Friguls, X. Joya, O. Garcia-Algar, C. R. Pallas, O. Vall and S. Pichini, *Anal. Bioanal. Chem.*, **2010,** *397*, 1157–1179.
11. C. Patel, M. Patel, S. Rani, M. Nivsarkar and H. Padh, *J. Chromatogr. B. Analyt. Technol. Biomed. Life Sci.*, **2007,** *850*, 356–360.

12. W. Guo, W. Li, G. Guo, J. Zhang, B. Zhou, Y. Zhai and C. Wang, *J. Chromatogr. B. Analyt. Technol. Biomed. Life Sci.*, **2007,** *854*, 128–134.
13. J. Teichert, J. B. Rowe, K. D. Ersche, N. Shandali, J. Sacher, A. Aigner and R. Regenthal, *Int. J. Clin. Pharmacol. Thre.*, **2020,** *58*, 426–438.
14. H.-J. Zhu, J.-S. Wang, J. L. Donovan, C. L. DeVane, B. B. Gibson and J. S. Markowitz, *J. Chromatogr. B. Analyt. Technol. Biomed. Life Sci.*, **2007,** *846*, 351–354.
15. B. Stegmann, A. Dörfelt and E. Haen, *Ther. Drug. Monit.*, **2016,** *38*, 98–107.
16. E. Papaseit, E. Marchei, M. Farre, O. Garcia-Algar, R. Pacifici and S. Pichini, *Drug Test. Anal.*, **2013,** *5*, 446–452.
17. E. Choong, S. Rudaz, A. Kottelat, D. Guillarme, J. L. Veuthey and C. B. Eap, *J. Pharm. Biomed. Anal.*, **2009,** *50*, 1000–1008.
18. J. H. Mullen, R. L. Shugert, G. D. Ponsler, Q. Li, B. Sundaram, H. L. Coales, J. E Yakupkovic, R. M. LeLacheur, W. J. Wheeler, F. J. Belas and J. M. Sauer, *J. Pharm. Biomed. Anal.*, **2005,** *38*, 720–733.
19. E. Marchei, E. Papaseit, O. Q. Garcia-Algar, M. Farre, R. Pacifici and S. Pichini, *J. Pharm. Biomed. Anal.*, **2012,** *60*, 26–31.
20. D. I. Appel, B. Brinda, J. S. Markowitz, J. H. Newcorn and H. J. Zhu, *Biomed. Chromatogr.*, **2012,** *26*, 1364–1370.
21. N. A. Farid, R. F. Bergstrom, E. A. Ziege, C. J. Parli and L. Lemberger, *J. Clin. Pharmacol.*, **1985,** *25*, 296–301.
22. A. Monfort, M. Jutras, B. Martin, I. Boucoiran, E. Ferreira and G. Leclair, *J. Pharm. Biomed. Analy.*, **2021,** *204*, 114236.
23. A. Alhmaunde, M. Masrournia and A. Javid, *Int. J. Env. Analy. Chem.*, **2023,** 1–19.
24. N. Kurnaz Yetim, M. M. Koç and D. Nartop, *J. Iran. Chem. Soc.*, **2022,** *19*, 2569–2580.
25. N. Kurnaz Yetim, F. Kurşun Baysak and M. M. Koç, *J. Nanostruct. Chem.*, **2021,** *11*, 589–599.
26. N. Kurnaz Yetim and E. Hasanoğlu Özkan, *J. Mater Sci: Mater Electron.*, **2021,** *32*, 24766–24774.
27. N. Kurnaz Yetim, F. Kurşun Baysak and M. M. Koç, *J. Mater. Sci. Mater. Electron.*, **2020,** 31, 18278–18288.
28. N. Kurnaz Yetim, E. Hasanoğlu Özkan and M. M. Koç, *Kırklareli University J. of Engineering and Sci.*, **2022,** *8*, 229–242.
29. European Medicines Agency (EMA)/Committee for Medicinal Products for Human Use (CHMP), Guideline on Bioanalytical Method Validation, EMA/CHMP, London, United Kingdom, 2011.
30. B. Ceylan, E. K. Tekkeli and C. Önal, *J. of Fluoresc.*, **2022,** *32*, 319–325